Supporting information for Metal-insulator crossover in monolayer MoS_2

I. Castillo, T. Sohier, M. Paillet, D. Cakiroglu, C. Consejo, C. Wen, F. Wasem Klein, M.-Q. Zhao, A. Ouerghi, S. Contreras, A.T. Charlie Johnson, M. Verstraete, B. Jouault, and S. Nanot

I. MOS_2 TRANSISTORS STUDIED IN THIS WORK

The optical images of M1, M2 and M3 analyzed in the main text are shown below after fabrication (and before measurements). The difference in color between the pictures comes from a different SiO_2 thickness ($\sim$ 290 nm for M1 and M2 and $\sim$ 330 nm for M3).

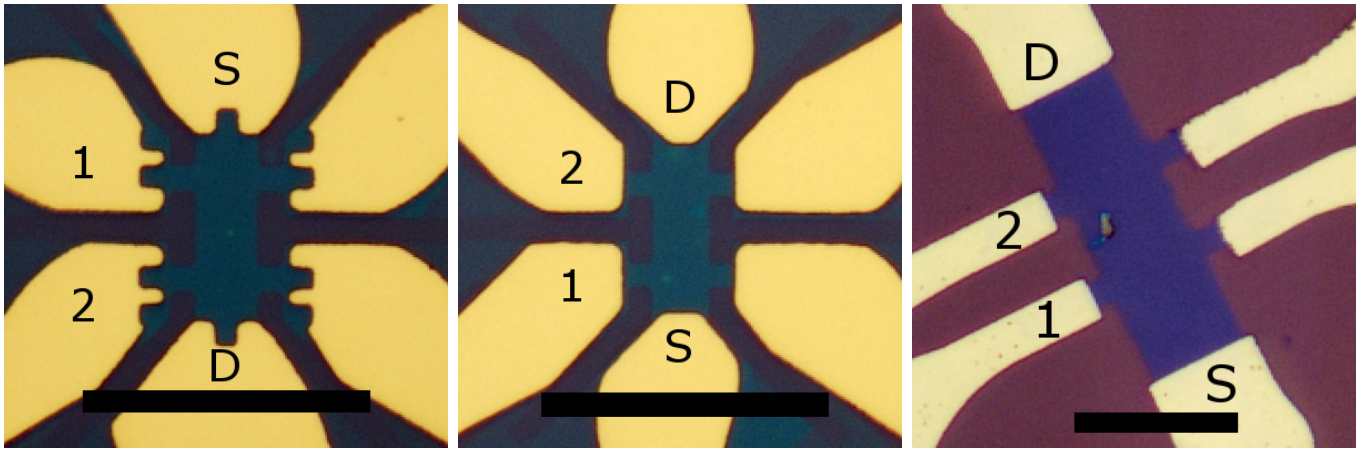

(a) (b) (c)

FIG. 1: Optical pictures of (a) M1, (b) M2 and (c) M3. Scale bar = 25 μm.

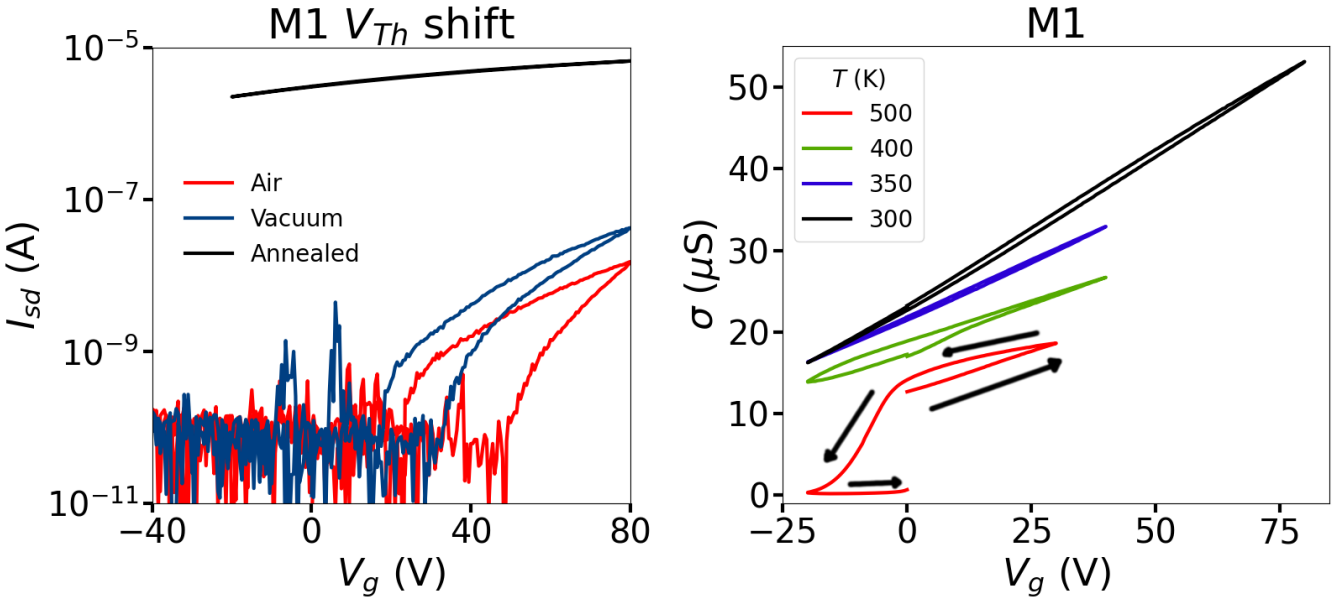

(a) (b)

FIG. 2: Conductivity of M1 *versus* gate voltage (a) at 300 K before the experiments in air (red), in vacuum (blue) and after annealing (black); (b) taken in vacuum during the cooling down process after an annealing at 600 K (down to 300 K). One can notice the hysteresis appearing for temperatures above 300 K, arrows indicate te sweeping direction.

II. EFFECT OF ANNEALING ON ELECTRON DENSITY AND HYSTERESIS

The thermal annealing considerably doped the samples with more electrons, as can be seen in Fig. 2a. The desorption of molecules from the sulphur vacancies leaves the dangling bond behind, which in turn acts as an electron donor. A difference in both hysteresis and threshold voltage is also noticed when going from air to vacuum, supporting the idea of desorption. The estimated change in doping with annealing for M1 device is $\sim 8 \times 10^{12}$ cm^{-2}.

Transfer curves measured during the cool down after annealing exhibit a high hysteresis at 500 K which tends to decrease when decreasing the temperature (Fig. 2b). A one-to-one comparison between the curves is difficult since the voltage range has been changed (due to a lower leakage current). Nevertheless, one can already see in this example that it becomes negligible below 350 K and that it remains around $\Delta V_{Th} \leq 10$ V.

III. EXTRACTING THE EFFECTIVE MOBILTY AND DOPING

In order to properly extract the carrier density and mobility of delocalized electrons in the conduction band, one has to be careful with contributions of localized electrons to the conductivity through hopping and thermal activation. Considering only band transport, the doping and mobility are given by $n_{2D} = C_{ox}(V_g - V_{Th})$ and $\mu = n_{2D}e/\sigma$ (as described in the main text), V_{Th} is the threshold voltage, C_{ox} is the SiO_2 capacitance.

One approach is to obtain the so-called FET mobility and V_{Th} by fitting the more linear part of the $\sigma(V_g)$ curves at high gate voltages (Fig. 3a). In this case the apparent V_{Th} varies from 17.5 V to -67 V between 20 K and 300 K. Alternatively, calculating the effective mobility, $\mu_{\text{eff}} = (\partial\sigma/\partial V_g)/C_{ox}$, by a direct derivation of these curves shows that μ is never perfectly constant even at high gate voltages (Fig. 3b). For the highest gate voltages used, one can see that μ_{eff} is increasing from ~ 40 cm^2/Vs at room temperature up to ~ 180 cm^2/Vs when phonon scattering becomes less efficient.

As discussed in the main text, we can then compare the carrier density, n_g, calculated using the temperature dependent V_{Th} with n_{eff}, the one obtained from μ_{eff}. Both approaches are expected to give a wrong value for low doping since both V_{Th} and μ_{eff} include contributions from VRH between localized states. Nevertheless, when accounting only for gate voltages $Vg > V_c$ (in the metallic regime), both approaches give similar results and succeed to include thermally activated carriers in the estimated carrier concentration.

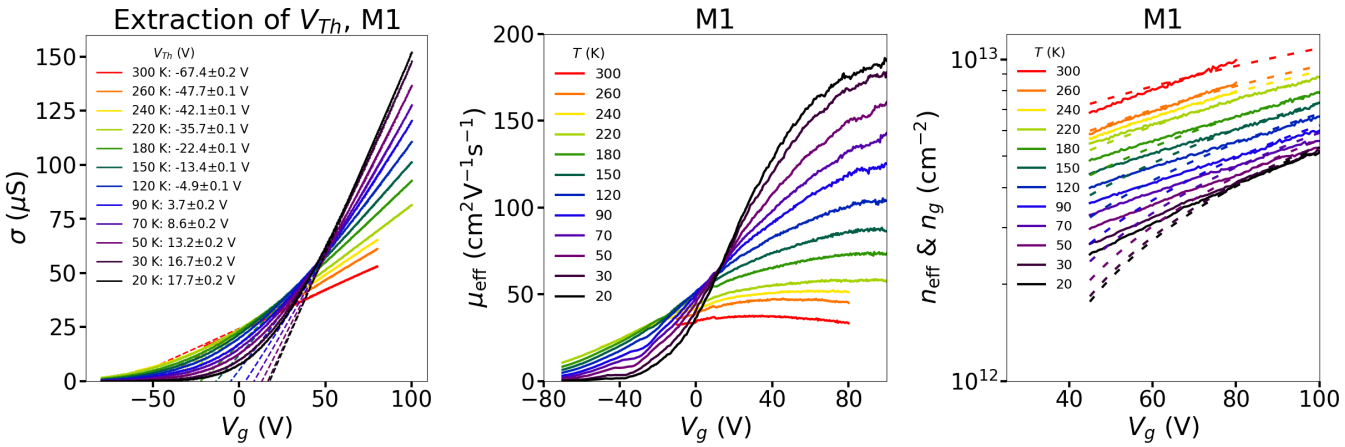

(a) (b) (c)

FIG. 3: (a) Conductivity versus gate voltage of device M1 (as in Fig. 3.a of the main text) between 300 K and 20 K, showing the linear fit (in dashed lines) used to extract a temperature dependent V_{Th}. (b) Effective mobility $\mu_{\text{eff}} = (\partial\sigma/\partial V_g)/C_{ox}$ versus gate voltage for the same measurements. (c) Carrier density versus gate voltage obtained from the previous analysis in (a) and (b), n_{eff} is in full lines and n_g is in dashed lines.

IV. M2'S CONDUCTIVITY AFTER A SECOND ANNEALING

Sample M2 was annealed twice at 600 K, performing the electrical measurements down to 20 K without exposing the sample to air. The data shown in the main text is after the first annealing (11 min), here we show the data after

the second annealing (26 min). The conductivity is lower and noisier than after the first annealing, suggesting the sample is being damaged by too long annealing process. Nevertheless, the overall trend is very similar between the two series of measurements. One can notice a sharp change in conductivity below 200 K because of the introduction of exchange gas (discussed below for M3).

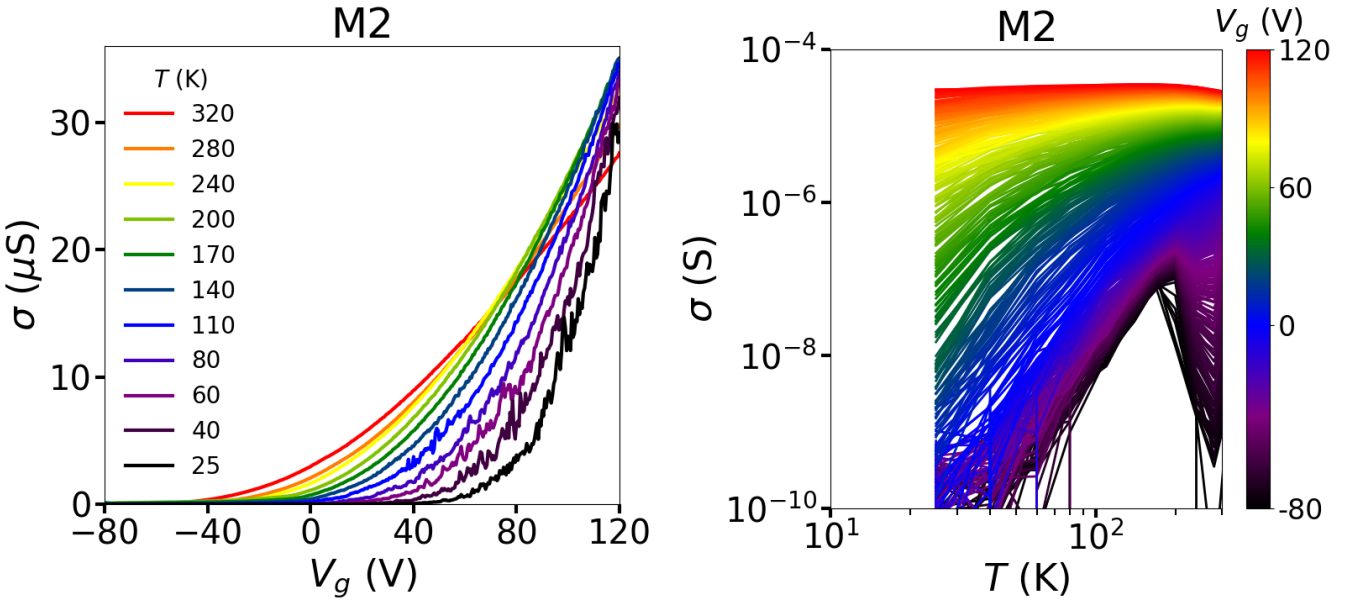

(a) (b)

FIG. 4: Conductivity of device M2 after the second annealing: (a) as a function of gate voltage, (b) as a function of temperature.

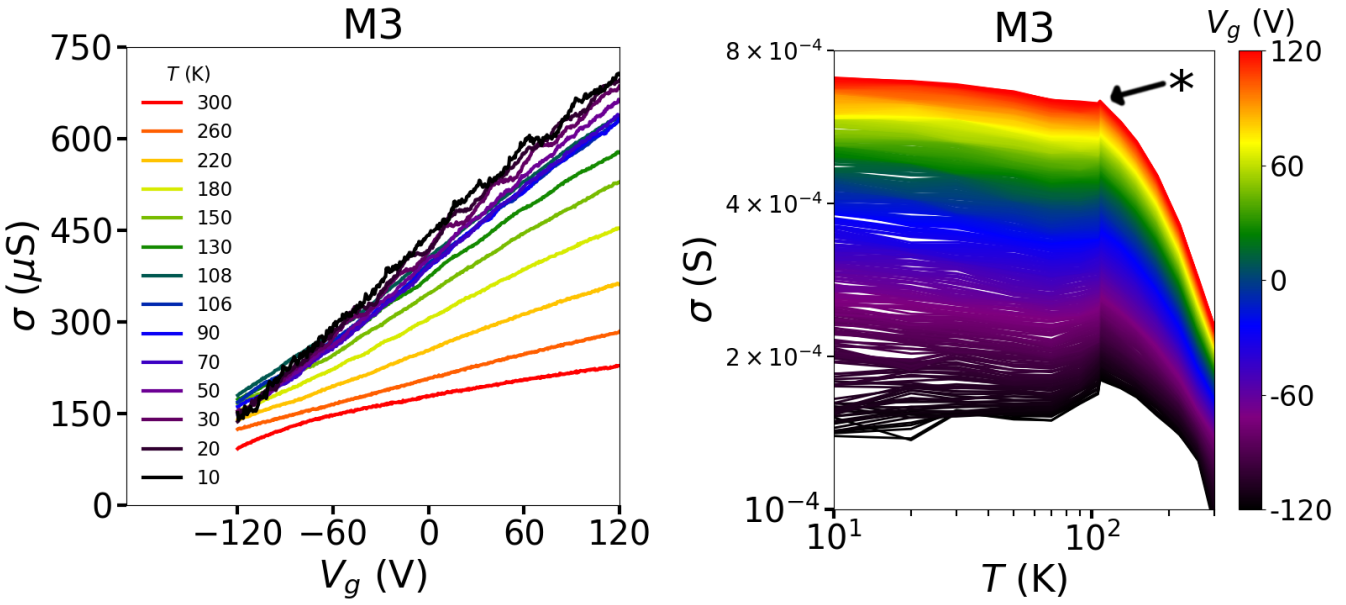

(a) (b)

FIG. 5: Conductivity of device M3: (a) as a function of gate voltage, (b) as a function of temperature.

V. M3'S CONDUCTIVITY

The change in conductivity with the introduction of exchange gas is more noticeable on this device. At $T = 108$ K (marked with an asterisk in Fig. 5b) the chamber was filled with He which was used as a heat exchange gas to cool the sample down to 20 K. As a result, the conductivity decreased and got noisier, with an apparent temperature-dependence suppression. This behavior was not observed in most of the other measurements (in particular M1 and M2 after the first annealing) and it is probably due to a pollution of the exchange gas line, MoS_2 being highly sensitive the environment.

VI. VRH MODEL: TEMPERATURE DEPENDENCE EXPONENT AND PREFACTOR

In Figure 4b of the main text (chapter IV.B), we introduce the dimensionless energy W and we plot W *vs.* T on a logarithmic scale to distinguish directly the exponent p^{-1} as the slope of this curve. In order to further confirm that $p = 2$ gives the best tendency compared to $p = 3$ for $V_g < -20$ V, (i) we have directly fitted this p-values from the $\ln(W)(\ln(T)$ curves, and (ii) we compared the fits based on different models.

In Figure 6a, the average p values for temperatures between 20 and 70 K extracted at given gate voltages are shown for device $M1$. The standard deviation is also given as a gray interval. At $V_g < -25$ V, $p = 2$ is indeed the best value as given by the fit ($V_{Th} \simeq 18$ V).

In Figure 6a, the conductivity is fitted as a function of $T^{-1/3}$ ($p = 3$) assuming a constant prefactor σ_0 or $\sigma_0 \propto T^{-1}$. These results can be directly compared with Figure 4c in the main text ($T^{-1/2}$ ($p = 2$ and σ_0 constant). When the fit is performed as a function of $T^{-1/3}$, the fitting lines cross very far from the vertical $T^{-1/p} = 0$ line. Moreover, the doping dependence of σ_0, which strongly increases when V_g (and the doping) decreases, has no physical explanation and has not been reported before.

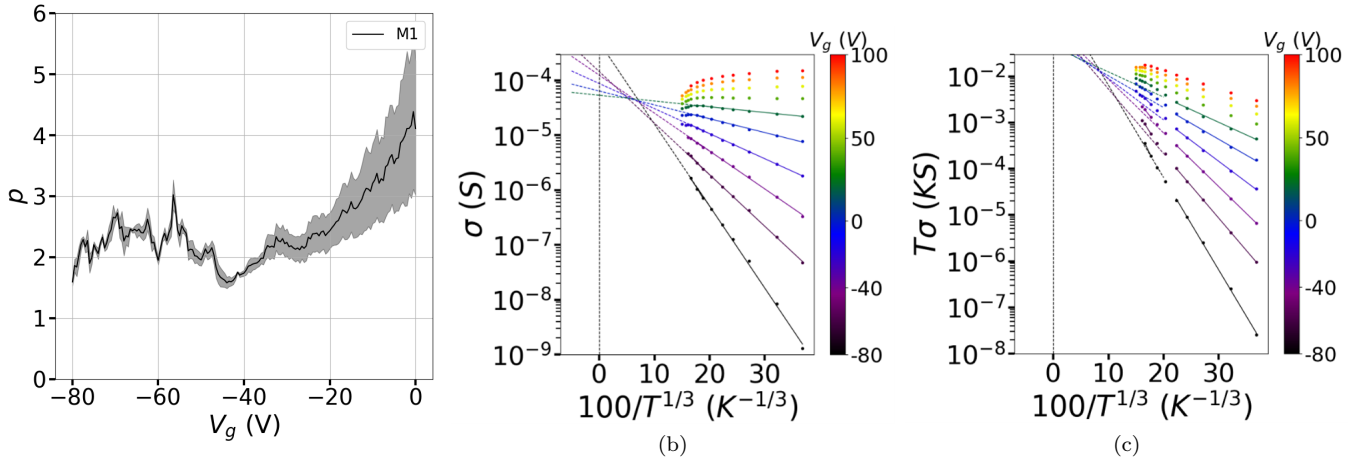

(a) (b) (c)

FIG. 6: (a) p-values obtained from fitting linearly the $\ln(W)(\ln(T)$ curves for device $M1$, the error bar is also reported as a gray region (corresponding to 1 standard deviation of the fits). (b) Linear fit of $\sigma(T^{-1/3})$ (c) Linear fit of $T\dot{\sigma}(T^{-1/3})$.

VII. LOCALIZATION LENGTH AND CHARACTERISTIC TEMPERATURES

Here, we show the hopping temperature T_2 and localization length ξ deduced from the ES VRH analysis described in the main text. One can clearly see in figure 7a that they vary by almost two orders of magnitude, reaching unreallistic values near de threshold voltage V_{Th}.

Finally, the conductivity of M_1 is plotted in Fig. 7b together with the transition points (V_c, σ_c) reprensented as dots and a solid black line. These data are compared with the three characteristic temperatures at play, in order to determine if a genuine MIT could occur as proposed by Das Sarma.[1] The Fermi temperature T_F defines the intrinsic temperature scale of the 2D electrons, the Bloch-Grüneisen temperature T_{BG} defines the characteristic temperature scale of phonon scattering, and the Dingle temperature T_D defines the cutoff of carrier screening by impurity disorder.

As a consequence, the temperature needed to observe a phase transition should respect the criteria:

$$T_D < T < T_F < T_{BG}$$

T_{BG} is calculated using the acoustic phonon velocity of $v_{ph} = 6.7 \times 10^3$ m/s; T_F and T_{BG} are obtained as a function of gate voltage using a capacitive model, and we used the mobilty at 20 K to determine T_D. One can see from those three dashed line that 1) a purely semi-classical transition is expected above 100 K, and 2) that according to these estimations one should not expect signatures of a quantum phase transition at any of the temperatures studied here. This makes the quality of the scaling even more surprising.

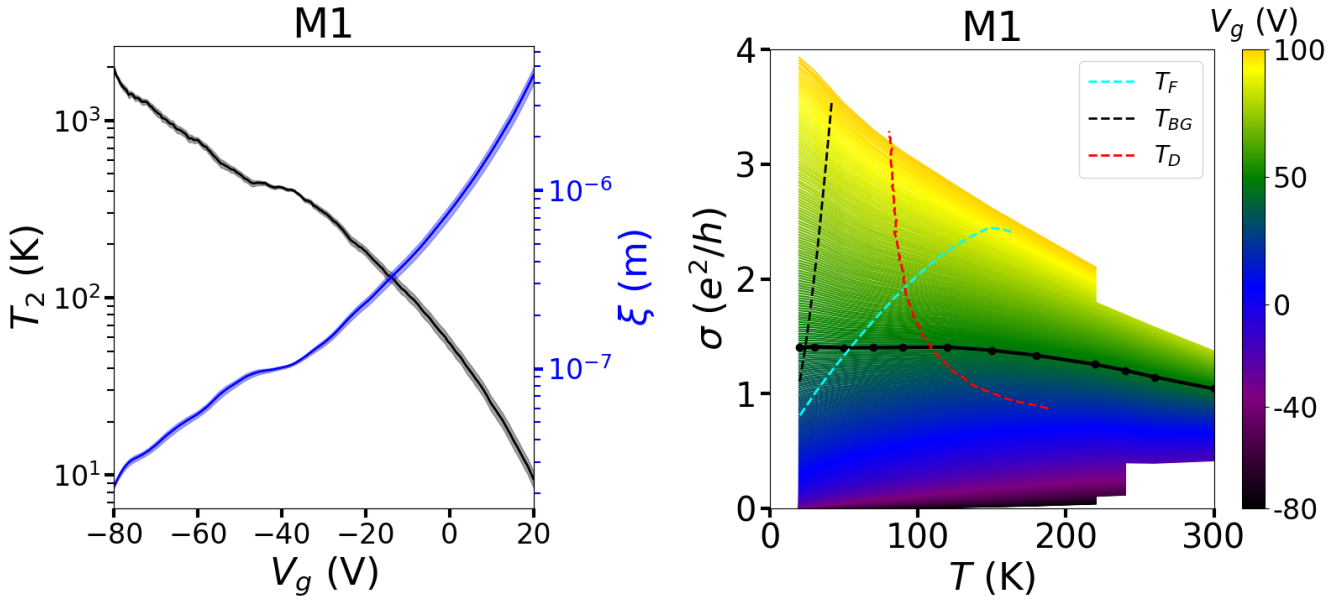

(a) (b)

FIG. 7: (a) Computed localization length (ξ) and extracted Efros-Shklovskii activation temperature (T_2) for M1 device. (b) Conductivity of device M1 in units e^2/h. The colored dashed lines show the limits of validity of a QPT arising purely from electronic effects. The solid black line is the curve used to scale the data into two branches.

[1] S. Das Sarma and E. H. Hwang, Scientific Reports **5**, 16655 (2015).